Inorganic Chemistry
Article

Inorg. Chem. **2010**, *49*, 3881–3887 **3881**
DOI: 10.1021/ic100061e

Magnetic and Structural Transitions at Dimerization of $C_{60}^{\bullet-}$ in Ionic Fullerene Complexes with Metalloporphyrins: $\{(TMP^{+})_2 \cdot M^{II}TPP\} \cdot (C_{60}^{-})_2 \cdot (C_6H_4Cl_2)_2 \cdot (C_6H_5CN)_2$ (M = Zn and Mn)

Dmitri V. Konarev,*,† Salavat S. Khasanov,‡ Guzeliya R. Mukhamadieva,† Leokadia V. Zorina,‡ Akihiro Otsuka,§ Hideki Yamochi,§ Gunzi Saito,⊥ and Rimma N. Lyubovskaya†

†*Institute of Problems of Chemical Physics RAS, Chernogolovka, Moscow region 142432, Russia,* ‡*Institute of Solid State Physics RAS, Chernogolovka, Moscow region 142432, Russia,* §*Research Center for Low Temperature and Materials Sciences, Kyoto University, Sakyo-ku, Kyoto 606-8501, Japan, and* ⊥*Research Institute, Meijo University, 1-501 Shiogamaguchi, Tempaku-ku, Nagoya 468-8502, Japan*

Received January 11, 2010

Ionic complexes containing $C_{60}^{\bullet-}$ radical anions and metalloporphyrins coordinatively bound to *N,N′,N′*-trimethylpiperazinium cations $\{(TMP^{+})_2 \cdot M^{II}TPP\} \cdot (C_{60}^{-})_2 \cdot (C_6H_4Cl_2)_2 \cdot (C_6H_5CN)_2$ [M = Zn (**1**) and Mn (**2**)] have been obtained. The crystal structures of **1** and **2** solved at 250 and 270 K, respectively, show layered packing in which fullerene layers alternate with the $(TMP^{+})_2 \cdot M^{II}TPP$ ones. Fullerenes form pairs in the layer with short center-to-center distances of 10.044 and 10.077 Å, respectively. The structures of **1** and **2** solved at 100 K indicate the formation of singly bonded $(C_{60}^{-})_2$ dimers. That results in the transition of **1** from the paramagnetic to diamagnetic state accompanied by the disappearance of the electron paramagnetic resonance (EPR) signal of $C_{60}^{\bullet-}$ at 220−150 K. Dimerization in **2** results in a decrease in the magnetic moment from 6.36 to 6.00 μ_B at 200−150 K and a change in the shape of EPR signal. The room-temperature EPR signal shows a major broad component at $g = 2.0678$ ($\Delta H = 111.6$ mT) attributed to both paramagnetic $C_{60}^{\bullet-}$ and high-spin $(TMP^{+})_2 \cdot Mn^{II}TPP$ species having strong exchange interaction. After dimerization, the signal is characteristic of isolated high-spin $Mn^{II}TPP$ ($g_\perp = 6$ with $|A| = 7.3$ mT and $g_{||} \approx 2$). Two TMP^{+} cations can coordinate to M^{II} in $(TMP^{+})_2 \cdot M^{II}TPP$. However, a weak coordination bond is formed only with one cation with the $M^{II} \cdots N(TMP^{+})$ distances of 2.489(2)−2.688(3) Å. As a result, metal atoms displace by ±0.232(3) Å (**1**, 250 K), ±0.231(1) Å (**1**, 100 K) and ±0.4684(7) Å (**2**, 270 K) out of the porphyrin plane to be located above and below the porphyrin plane with equal occupancies for both positions. The symmetry of the crystal structure of **2** decreases from monoclinic to triclinic under cooling. That results in unequal 0.85/0.15 occupation of the Mn^{II} positions at 100 K with displacement of the metal by 0.391(2) and 0.554(4) Å, respectively.

Introduction

Complexes of fullerenes with metalloporphyrins are of great interest. Neutral complexes were obtained mainly with metal octaethyl- ($M^{II}OEP$) or tetraphenylporphyrins ($M^{II}TPP$), which cocrystallized with fullerenes C_{60} and C_{70}[1] as well as fullerene derivatives,[1a,2] endometallofullerenes[3] and higher fullerenes.[4] These cocrystals were used to determine precise molecular structures of fullerenes.[1−4]

Metalloporphyrins can also be involved in ionic complexes with fullerenes. This can be performed by the direct reduction

*To whom correspondence should be addressed. E-mail: konarev@icp.ac.ru. Fax: +007-496-522-18-52.

(1) (a) Olmstead, M. M.; Costa, D. A.; Maitra, K.; Noll, B. C.; Phillips, S. L.; Van Calcar, P. M.; Balch, A. L. *J. Am. Chem. Soc.* **1999**, *121*, 7090. (b) Yudanova, E. I.; Konarev, D. V.; Gumanov, L. L.; Lyubovskaya, R. N. *Russ. Chem. Bull.* **1999**, *48*, 718. (c) Boyd, P. D. W.; Hodgson, M. C.; Chaker, L.; Rickard, C. E. F.; Oliver, A. G.; Brothers, P. J.; Bolskar, R.; Tham, F. S.; Reed., C. A. *J. Am. Chem. Soc.* **1999**, *121*, 10487. (d) Konarev, D. V.; Neretin, I. S.; Slovokhotov, Yu. L.; Yudanova, E. I.; Drichko, N. V.; Shuga, Yu. M.; Tarasov, B. P.; Gumanov, L. L.; Batsanov, A. S.; Howard, J. A. K.; Lyubovskaya, R. N. *Chem.—Eur. J.* **2001**, *7*, 2605. (e) Konarev, D. V.; Kovalevsky, A. Yu.; Li, X.; Neretin, I. S.; Litvinov, A. L.; Drichko, N. V.; Slovokhotov, Yu. L.; Coppens, P.; Lyubovskaya, R. N. *Inorg. Chem.* **2002**, *41*, 3638. (f) Boyd, P. D. W.; Reed, C. A. *Acc. Chem. Res.* **2005**, *36*, 235. (g) Ishii, T.; Aizawa, N.; Kanehama, R.; Yamashita, M.; Sugiura, K.; Miyasaka, H. *Coord. Chem. Rev.* **2002**, *226*, 113.

(2) Zheng, M.; Li, F.; Shi, Z.; Gao, Y.; Kadish, K. M. *J. Org. Chem.* **2007**, *72*, 2538.

(3) (a) Stevenson, S.; Rice, G.; Glass, T.; Harich, K.; Cromer, F.; Jordan, M. R.; Craft, J.; Hadju, E.; Bible, R.; Olmstead, M. M.; Maitra, K.; Fisher, A. J.; Balch, A. L.; Dorn., H. C. *Nature* **1999**, *401*, 55. (b) Olmstead, M. M.; de Bettencourt-Dias, A.; Stevenson, S.; Dorn, H. C.; Balch, A. L. *J. Am. Chem. Soc.* **2002**, *124*, 4172.

(4) (a) Epple, L.; Amsharov, K.; Simeonov, K.; Dix, I.; Jansen, M. *Chem. Commun.* **2008**, 5610. (b) Epple, L.; Amsharov, K.; Jansen, M. *Fullerenes, Nanotubes, Carbon Nanostruct.* **2009**, *17*, 67.

(5) (a) Pénicaud, A.; Hsu, J.; Reed, C. A.; Koch, A.; Khemani, K. C.; Allemand, P.-M.; Wudl, F. *J. Am. Chem. Soc.* **1991**, *113*, 6698. (b) Stinchcombe, J.; Pénicaud, A.; Bhyrappa, P.; Boyd, P. D. W.; Reed, C. A. *J. Am. Chem. Soc.* **1993**, *115*, 5212.

Published on Web 03/24/2010

Scheme 1

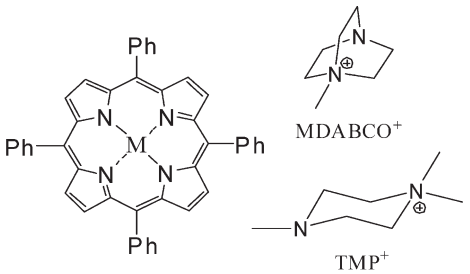

$M^{II}TPP$ (M = Zn and Mn)

of fullerenes by metalloporphyrins such as $Cr^{II}TPP$ or $Sn^{II}TTolP$ (TTolP = tetratolylporphyrin) in the presence of coordinating ligands.[5] However, most of metalloporphyrins are weak donors that do not reduce fullerenes and form neutral complexes only.[1] Another way is the insertion of metalloporphyrins into the ionic fullerene $(D_1^+)\cdot(C_{60}^{\bullet-})$ complexes through the formation of a coordination bond between metalloporphyrin and a nitrogen-containing cation (D_1^+). Metalloporphyrins containing M = Zn^{II}, Co^{II}, Mn^{II}, and Fe^{II} capable of extra coordination can be used for these purposes. Positively charged $(D_1^+)_n\cdot(M^{II}porphyrin)$ (n = 1 or 2) assemblies formed in solution can be further cocrystallized with mono- or dianions of fullerenes to form $\{(D_1^+)_x\cdot M^{II}porphyrin\}\cdot(C_{60}^{n-})_x$ (x, n = 1 or 2).[6] Now only the *N*-methyldiazabicyclooctanium cation ($MDABCO^+$; Scheme 1) was used in the synthesis of such complexes. The $MDABCO^+$ cation is a strongly coordinating monodentate ligand with one free nitrogen atom accessible to coordination. Metal tetraphenylporphyrins form assemblies with two cations per porphyrin molecule: $\{(MDABCO^+)_2\cdot M^{II}TPP\}$(M = Zn, Co, Mn, and Fe), and correspondingly metal atoms are six-coordinated in these porphyrins. In a series of complexes with the $\{(MDABCO^+)_2\cdot M^{II}TPP\}$ units, C_{60} anions form one-dimensional chains with antiferromagnetic interaction of the spins, C_{60}^{2-} dianions are isolated, and C_{70} anions form diamagnetic singly bonded $(C_{70}^-)_2$ dimers.[6a,b] Only one cation coordinates to metal tetrakis(methoxyphenyl)-porphyrins ($M^{II}TMPP$) and $M^{II}OEP$ to form $\{(MDABCO^+)\cdot M^{II}TMPP\}$ (M = Co^{II}) and $\{(MDABCO^+)\cdot M^{II}OEP\}$ (M = Zn, Co, Mn, and Fe). Fullerene anions are located from the opposite side of the porphyrin macrocycle without coordination (except complex with $Co^{II}OEP$[6d]). Thus, metals in porphyrins are five-coordinated. Paramagnetic doubly bonded $(C_{60}^-)_2$ dimers[6c] and diamagnetic σ-bonded $\{(MDABCO^+)\cdot CoOEP\cdot(C_{60}^-)\}$ or $\{Co^{II}OEP\cdot(C_{60}^-)\}$ assemblies[6d,e] are formed in these complexes.

In this work, we newly used the *N*,*N*′,*N*′-trimethylpiperazinium cation (TMP^+; Scheme 1) to synthesize ionic complexes of metalloporphyrins with fullerenes. *N*,*N*′-Dimethylpiperazine (DMP) is a bidentate ligand. DMP forms binuclear coordination structures with $Zn^{II}TPP$ and $Mn^{II}TPP$, which were cocrystallized with fullerenes in molecular and ionic complexes.[7] The addition of 1 equiv of MeI to DMP produces a monodentate TMP^+ cation with one free nitrogen atom accessible for coordination. Two $\{(TMP^+)_2\cdot M^{II}TPP\}\cdot(C_{60}^-)_2\cdot(C_6H_4Cl_2)_2\cdot(C_6H_5CN)_2$ [M = Zn (**1**) and Mn (**2**)] complexes were obtained, and their crystal structures were determined from X-ray diffraction on a single crystal at 250 (270) and 100 K. Dimerization of $C_{60}^{\bullet-}$ is observed in both complexes, reversibly changing their magnetic properties. The unusual geometry is observed for the coordination of $(TMP^+)_2\cdot M^{II}TPP$ assemblies. The metal atoms are in a six-coordinated environment. Nevertheless, they displace toward only one cation to form five-coordinated metal species and locate above and below the porphyrin plane. The observed splitting of the metal position corresponds to the averaging of two possible configurations over the crystal.

Experimental Section

Materials. Zinc(II) tetraphenylporphyrin ($Zn^{II}TPP$), manganese(III) tetraphenylporphyrin chloride ($Mn^{III}TPPCl$), sodium borohydride ($NaBH_4$), sodium ethanethiolate (CH_3CH_2SNa), *N*,*N*′-dimethylpiperazine (DMP), and methyl iodide (CH_3I) were purchased from Aldrich. $Mn^{II}TPP$ was obtained by the reduction of $Mn^{III}TPPCl$ by $NaBH_4$ in ethanol.[8] C_{60} of 99.98% purity was purchased from MTR Ltd. Solvents were purified in an argon atmosphere. *o*-Dichlorobenzene ($C_6H_4Cl_2$) was distilled over CaH_2 under reduced pressure, benzonitrile (C_6H_5CN) was distilled over sodium under reduced pressure, and hexane was distilled over sodium benzophenone. The solvents were degassed and stored in a glovebox. All manipulations for the synthesis of air-sensitive **1** and **2** were carried out in a MBraun 150B-G glovebox with a controlled atmosphere and contents of H_2O and O_2 of less than 1 ppm. The crystals were stored in the glovebox and sealed in 2 mm quartz tubes for electron paramagnetic resonance (EPR) and SQUID measurements under 10^{-5} Torr. KBr pellets for IR and UV−visible−near-IR (NIR) measurements were prepared in the glovebox.

Synthesis. *N*,*N*′,*N*′-Trimethylpiperazinium iodide ($TMP\cdot I$) was obtained by the dropwise addition of CH_3I (2.5 mL, 0.04 mol) to DMP (6.8 mL, 0.05 mol) dissolved in 20 mL of acetonitrile upon stirring. A white crystalline precipitate of $TMP\cdot I$ formed immediately. After 2 h of stirring, the precipitate was filtered off, washed with two portions of 5 mL of acetonitrile, and dried in a vacuum for 8 h. A total of 8.4 g of $TMP\cdot I$ was obtained with 80% yield.

The crystals of $\{(TMP)_2\cdot Zn^{II}TPP\}\cdot(C_{60})_2\cdot(C_6H_4Cl_2)_2\cdot(C_6H_5CN)_2$ (**1**) were obtained by the following procedure. C_{60} (25 mg, 0.035 mmol), a 10-fold molar excess of CH_3CH_2SNa (30 mg, 0.36 mmol), a 5-fold molar excess of $TMP\cdot I$ (44.5 mg, 0.175 mmol), and $Zn^{II}TPP$ (24 mg, 0.035 mmol) were stirred in 10 mL of the $C_6H_4Cl_2/C_6H_5CN$ (8:2) mixture for 4 h at 60 °C. During stirring, the color of the solution changed from violet to red-brown. The solution was cooled down to room temperature and filtered. The NIR spectrum was measured to indicate the selective reduction of C_{60} to a 1− charged state. A total of 4 mL of $C_6H_4Cl_2$ was added, the solution was filtered into a 50 mL glass tube of 1.8 cm diameter with a ground-glass plug, and 25 mL of hexane was layered over the solution. Diffusion was carried out for 1 month to give crystals of **1** on the wall of the tube. The solvent was decanted from the crystals, which were then washed with hexane (yield 70%). The crystals were black parallelograms with a characteristic blue luster and up to $2 \times 1 \times 0.5$ mm^3 in size.

The crystals of $\{(TMP)_2\cdot Mn^{II}TPP\}\cdot(C_{60})_2\cdot(C_6H_4Cl_2)_2\cdot(C_6H_5CN)_2$ (**2**) were obtained similarly. Instead of $Zn^{II}TPP$,

(6) (a) Konarev, D. V.; Khasanov, S. S.; Otsuka, A.; Saito, G.; Lyubovskaya., R. N. *Inorg. Chem.* **2007**, *46*, 2261. (b) Konarev, D. V.; Khasanov, S. S.; Saito, G.; Lyubovskaya, R. N. *J. Porphyrins Phthalocyanines* **2008**, *12*, 1146. (c) Konarev, D. V.; Khasanov, S. S.; Otsuka, A.; Saito, G.; Lyubovskaya., R. N. *J. Am. Chem. Soc.* **2006**, *128*, 9292. (d) Konarev, D. V.; Khasanov, S. S.; Otsuka, A.; Saito, G.; Lyubovskaya, R. N. *Chem.—Eur. J.* **2006**, *12*, 5225. (e) Konarev, D. V.; Khasanov, S. S.; Saito, G.; Lyubovskaya, R. N. *Cryst. Growth Des.* **2009**, *9*, 1170. (f) Konarev, D. V.; Lyubovskaya, R. N. *Macroheterocycles* **2009**, *2*, 191.

(7) Konarev, D. V.; Khasanov, S. S.; Saito, G.; Otsuka, A.; Lyubovskaya, R. N. *Inorg. Chem.* **2007**, *46*, 7601.

(8) Wayland, B. B.; Olson, L. W.; Siddiqui, Z. U. *J. Am. Chem. Soc.* **1970**, *92*, 4235.

Table 1. X-ray Diffraction Data for **1** and **2**

compound	{ZnTPP·(TMP)$_2$}·(C$_{60}$)$_2$·(C$_6$H$_4$Cl)$_2$·(C$_6$H$_5$CN)$_2$		{MnTPP·(TMP)$_2$}·(C$_{60}$)$_2$·(C$_6$H$_4$Cl)$_2$·(C$_6$H$_5$CN)$_2$		
temperature, K	100(2)	250(2)	100(2)	200(2)	270(2)
empirical formula	C$_{204}$H$_{80}$Cl$_4$N$_{10}$Zn		C$_{204}$H$_{80}$Cl$_4$N$_{10}$Mn		
M_r [g·mol^{-1}]	2877.95		2867.52		
cryst color and shape size, mm × mm × mm	black prism 0.35 × 0.30 × 0.25		black prism 0.40 × 0.30 × 0.25		
cryst syst	monoclinic	monoclinic	triclinic	monoclinic	monoclinic
space group	*C*2/*c*	*C*2/*c*	$C\bar{1}$	*C*2/*c*	*C*2/*c*
a, Å	28.658(3)	28.443(3)	28.5037(13)	28.365(3)	28.5555(19)
b, Å	15.0186(10)	15.3633(8)	15.3623(6)	15.4664(8)	15.3559(11)
c, Å	30.522(9)	30.787(7)	30.1121(13)	30.563(8)	30.951(2)
α, deg	90	90	90.173(4)	90	90
β, deg	110.475(14)	110.261(12)	109.828(4)	110.072(13)	110.348(8)
γ, deg	90	90	89.514(5)	90	90
V, Å^3	12307(4)	12621(3)	12403.4(9)	12594(3)	12725.1(15)
Z	4	4	4	4	4
ρ_{calcd} [g·cm^{-3}]	1.553	1.515	1.536	1.512	1.497
μ [mm^{-1}]	0.363	0.354	0.268	0.264	0.262
F(000)	5888	5888	5868	5868	5868
abs corrn min/max transmn	multiscan	multiscan	multiscan	multiscan	multiscan
	0.87	0.85	0.91	0.90	0.90
	0.93	0.92	0.95	0.96	0.97
max 2*θ*, deg	56.56	56.56	56.56	56.56	56.56
reflns measd	56133	75387	54511	50649	85067
unique reflns	15190	15417	30499	14906	15450
param restraints	1536	1350	2802	925	1350
	1739	2247	3736	687	2266
reflns [$F_o > 2\sigma F_o$]	10442	7887	24854	8932	8103
R1 [$F_o > 2\sigma F_o$]	0.0705	0.0772	0.0674	0.0752	0.0760
wR2 (all data)[a]	0.2128	0.2540	0.1808	0.2442	0.2743
a	0.1244	0.1328	0.1012	0.1253	0.1669
b	19.9883	6.8397	18.5569	9.0137	0.0315
GOF	1.027	1.050	1.017	1.106	1.078
restr. GOF	0.976	1.020	0.982	1.103	1.068
CCDC number	761078	761077	761081	761080	761079

[a] $w = 1/[\sigma^2(F_o^2) + (aP)^2 + bP]$, where $P = [\max(F_o^2,0) + 2F_c^2]/3$.

$Mn^{II}TPP$ was used. Diffusion was carried out for 1 month to give crystals of **2** on the wall of the tube. The solvent was decanted from the crystals, which were then washed with hexane (yield 62%). The crystals were black parallelograms with a characteristic blue luster and up to 1 × 0.5 × 0.3 mm^3 in size.

The composition of the complexes was determined from X-ray structural analysis on a single crystal. Several crystals tested from the synthesis have the same unit cell parameters to show the presence of the only phase. The composition of the complexes was supported by elemental analysis. Calcd for C$_{204}$H$_{80}$Cl$_4$N$_{10}$Zn (**1**, 2877.95): C, 85.16; H, 2.78; N, 4.86; Cl, 4.93; Zn, 2.27. Found: C, 86.12; H, 2.95; N, 4.81. Calcd for C$_{204}$H$_{80}$Cl$_4$N$_{10}$Mn (**2**, 2867.52): C, 85.47; H, 2.79; N, 4.87; Cl, 4.95. Found: C, 85.69; H, 2.81; N, 4.96; Cl, 4.51. Mn, 1.92.

General Procedures. UV−visible−NIR spectra were measured in KBr pellets on a Shimadzu 3100 spectrometer in the 240−2600 nm range. FT-IR spectra were measured in KBr pellets with a Perkin-Elmer 1000 Series spectrometer (400−7800 cm^{-1}). EPR spectra were recorded from 4 up to 293 K with a JEOL JES-TE 200 X-band ESR spectrometer equipped with a JEOL ES-CT470 cryostat. A Quantum Design MPMS-XL SQUID magnetometer was used to measure the static susceptibility of polycrystalline **1** and **2** between 1.9 and 300 K in a 100 mT static magnetic field. A sample-holder contribution and core-temperature-independent diamagnetic susceptibility (χ_0) were subtracted from the experimental values. The χ_0 values for **1** ($\chi_0 = -1262 \times 10^{-6}$ emu·mol^{-1}) and **2** ($\chi_0 = -1257 \times 10^{-6}$ emu·mol^{-1}) were calculated using the Pascal constants. The values of -252×10^{-6} emu·mol^{-1} for C$_{60}$,[9] -440×10^{-6} emu·mol^{-1} for $Zn^{II}TPP$, -430×10^{-6} emu·mol^{-1} for $Mn^{II}TPP$, -85×10^{-6} emu·mol^{-1} for TMP^+, -83×10^{-6} emu·mol^{-1} for C$_6$H$_4$Cl$_2$, and -65×10^{-6} emu·mol^{-1} for C$_6$H$_5$CN were used. The values of θ and C for **1** and **2** below dimerization were calculated using experimental data in the 10−140 K range: $\chi_M = C/(T - \theta) + \chi_0$. The magnetic moment ($\mu_{eff}$) was calculated with an appropriate formula: $\mu_{eff} = (8\chi_M T)^{1/2}$.

Crystal Structure Determination. X-ray diffraction data for **1** at 250(2) and 100(2) K and for **2** at 270(2), 200(2), and 100 (2) K are listed in Table 1. The intensity data were collected on an Oxford diffraction "Gemini-R" CCD diffractometer with graphite-monochromated Mo Kα radiation at low temperatures using an Oxford Instrument Cryojet system. Raw data reduction to F^2 was carried out using CrysAlisPro, Oxford Diffraction Ltd. The structures were solved by direct methods and refined by the full-matrix least-squares method against F^2 using *SHELX-97*.[10] Non-hydrogen atoms were refined in the anisotropic approximation. The positions of the hydrogen atoms were calculated geometrically. Subsequently, the positions of the hydrogen atoms were refined by the "riding" model with $U_{iso} = 1.2U_{eq}$ of the connected non-hydrogen atom or as ideal CH_3 groups with $U_{iso} = 1.5U_{eq}$.

Molecular Disorder in 1 and 2. The crystal structure of **1** at 250 K contains $C_{60}^{\bullet-}$ radical anions disordered between two orientations with 0.879(3)/0.121(3) occupancies. C$_6$H$_4$Cl$_2$ molecules are disordered among three orientations. At 100 K, the $(C_{60}^-)_2$ dimers are disordered between two orientations with 0.9177(16)/0.0823(16) occupancies. All other components are ordered.

The crystal structure of **2** at 270 K contains $C_{60}^{\bullet-}$ radical anions disordered between two orientations with 0.790(3)/0.210(3) occupancies. A temperature decrease down to 200 K orders $C_{60}^{\bullet-}$. There are two crystallographically independent $(C_{60}^-)_2$ dimers in the triclinic unit cell of **2** at 100 K. One dimer is ordered, and the other dimer is disordered between two orientations with 0.718(2)/0.282(2) occupancies. C$_6$H$_4$Cl$_2$ molecules are

(9) Ruoff, R. S.; Beach, D.; Cuomo, J.; McGuire, T.; Whetten, R. L.; Diederich, F. *J. Phys. Chem.* **1991**, *95*, 3457.

(10) Sheldrick, G. M. *SHELX97*; University of Göttingen: Göttingen, Germany, **1997**.

disordered in the crystal structure of **2** at all temperatures. However, all other components are ordered.

To keep the fullerene geometry close to ideal in the disordered groups, bond-length restraints were applied along with the next-nearest-neighbor distances, using the SADI SHELXL instruction. To keep the anisotropic thermal parameters of the fullerene atoms within reasonable limits, the displacement components were restrained using ISOR and DELU SHELXL instructions. That results in a great number of restraints used for the refinement of the crystal structures of **1** and **2**.

Results and Discussion

a. Synthesis. To prepare **1** and **2**, we reduced fullerene C_{60} with CH_3CH_2SNa in the presence of metalloporphyrin and an excess of TMP·I in the $C_6H_4Cl_2/C_6H_5CN$ (8:2) mixture. Then 4 mL of $C_6H_4Cl_2$ was added, and the diffusion of hexane into the obtained solution during 1 month gave the crystals of the complexes. Because the $(TMP^+)\cdot(C_{60}^{\bullet-})$ salt did not form crystals (no crystals are formed without $M^{II}TPP$), the ionic complex containing metalloporphyrin could be obtained selectively. The composition of $\{(TMP)_2\cdot M^{II}TPP\}\cdot(C_{60})_2\cdot(C_6H_4Cl_2)_2\cdot(C_6H_5CN)_2$ [M = Zn (**1**) and Mn (**2**)] was determined from X-ray diffraction data on a single crystal.

b. Optical Properties. The IR and UV−visible−NIR spectra of **1** and **2** are given in the Supporting Information. Four absorption bands of C_{60} are observed in the spectra of the complexes at 525, 575−576, 1176, and 1389 cm^{-1}. The position of the absorption band of $F_{1u}(4)$ mode at 1389 cm^{-1} corresponds to the 1− charged state of C_{60}.[11] The increase in the band intensity at 575−576 cm^{-1} relative to that at 525 cm^{-1} also indicates a 1− charge on C_{60}.[11b] The positions of the peaks in the UV−visible−NIR spectra of **1** and **2** are listed in Table 2. Both complexes manifest bands in the NIR range characteristic of the $C_{60}^{\bullet-}$ radical anions near 950 and 1080 nm.[11] The Soret and Q bands of porphyrins are observed in the visible range. Because the position of the Soret band is sensitive to coordination of the ligand to the central metal atoms, the shift of these bands by 5−6 nm to the red side (Table 2) can be associated with weak coordination of TMP^+ to metalloporphyrins.

c. Crystal Structures of 1 and 2. Complexes **1** and **2** have similar compositions and are isostructural. At 250 (270) K, their unit cell is monoclinic and contains monomeric $C_{60}^{\bullet-}$ radical anions. They are disordered between two orientations. Figures are shown and distances were calculated only for major [88% (**1**) and 79% (**2**)] occupied orientations of $C_{60}^{\bullet-}$.

The complexes have layered structures. Fullerene layers (Figure 1a,b) lie parallel to the *bc* plane and alternate with the $(TMP^+)_2\cdot M^{II}TPP$ layers. Fullerenes form pairs within the layers (marked by arrows in Figure 1b). The center-to-center distance between fullerenes in the pairs is 10.044 Å in **1** and 10.077 Å in **2**, and several short van der Waals (VdW) C···C contacts are formed between them (3.156−3.339 Å). The center-to-center distances with two other fullerene neighbors in the layer are 10.435 and 10.409 Å, respectively. In this case, no interfullerene VdW C···C contacts are formed. Fullerene layers contain large elongated hexagonal vacancies occupied by benzonitrile molecules (Figure 1b). Two TMP^+ cations from the $(TMP^+)_2\cdot M^{II}TPP$ layers located above and below the fullerene layer are also arranged in these vacancies (Figure 1a). There are only several H-$(TMP^+)\cdots C(C_{60}^-)$ contacts in the 2.7−2.8 Å range and one VdW $C(M^{II}TPP)\cdots C(C_{60}^-)$ contact between fullerene and $(TMP^+)_2\cdot M^{II}TPP$ layers. Therefore, the structure is held together mainly by electrostatic forces between negatively charged fullerene and positively charged $(TMP^+)_2\cdot M^{II}TPP$ layers.

Table 2. UV−Visible−NIR Spectra of Parent Compounds and Complexes **1** and **2**

	porphyrin		fullerene	
compound	Soret band, nm (shift, nm)	Q bands, nm	UV−visible range	NIR range
C_{60}			341, 470	
$Zn^{II}TPP$	431	553, 596, 623		
$Mn^{II}TPP$	443	−, 572, 611		
1	437 (6)	562, 602, −	−, 335	947, 1082
2	448 (5)	−, 574, 613	−, 338	950, 1080

The crystal structure of **2** was studied at 200 K. It contains monomeric $C_{60}^{\bullet-}$ radical anions that are completely ordered at this temperature.

The crystal structures of **1** and **2** at 100(2) K contain singly bonded $(C_{60}^-)_2$ dimers (Figure 1c,d). They are disordered between two orientations. Figures are shown and distances were calculated only for major [92% (**1**) and 72% (**2**)] occupied orientations of $(C_{60}^-)_2$. Thus, dimerization occurs in the complexes between 250 and 100 K for **1** and between 200 and 100 K for **2**. Dimers have C_{2h} symmetry. The length of the intercage C−C bond is 1.588(4) Å, and the center-to-center interfullerene distance is 9.320 Å for the ordered $(C_{60}^-)_2$ dimer in **2**. A similar geometry was observed for other single-bonded $(C_{60}^-)_2$ dimers.[12] Dimerization is realized, namely, in the fullerene pairs with the shortest center-to-center distance (Figure 1b,d, arrows) because the VdW C···C contacts between fullerenes are observed only within these pairs. The monoclinic unit cell is retained at dimerization in **1**. However, a transition from the monoclinic to triclinic unit cell is observed in **2**.

The molecular structure of the $(TMP^+)_2\cdot Zn^{II}TPP$ assembly at 250 K is shown in Figure 2a (Table 3). The Zn^{II} atoms displace by ±0.232(3) Å out of the porphyrin plane to be located above and below this plane with equal probability. For each position, one $Zn^{II}-N(TMP^+)$ distance is short [2.688(3) Å], indicating weak coordination of a free nitrogen atom of TMP^+ to $Zn^{II}TPP$. The $Zn^{II}\cdots N(TMP^+)$ distance with the second TMP^+ cation is long [3.149(4) Å], indicating the absence of coordination. Therefore, only one of two TMP^+ cations coordinates to $Zn^{II}TPP$, and zinc atoms are

(11) (a) Semkin, V. N.; Spitsina, N. G.; Krol, S.; Graja, A. *Chem. Phys. Lett*. **1996**, *256*, 616. (b) Picher, T.; Winkler, R.; Kuzmany, H. *Phys. Rev. B* **1994**, *49*, 15879. (c) Konarev, D. V.; Lyubovskaya, R. N. *Russ. Chem. Rev*. **1999**, *68*, 19. (d) Reed, C. A.; Bolskar, R. D. *Chem. Rev*. **2000**, *100*, 1075.

(12) (a) Konarev, D. V.; Khasanov, S. S.; Otsuka, A.; Saito, G. *J. Am. Chem. Soc*. **2002**, *124*, 8520. (b) Konarev, D. V.; Khasanov, S. S.; Kovalevsky, A. Yu.; Saito, G.; Otsuka, A.; Lyubovskaya, R. N. *Dalton Trans*. **2006**, 3716. (c) Schulz-Dobrick, M.; Jansen, M. *Angew. Chem., Int. Ed*. **2008**, *47*, 2256. (d) Domrachev, G. A.; Shevelev, Yu. A.; Cherkasov, V. K.; Markin, G. V.; Fukin, G. K.; Khorshev, S. Ya.; Kaverin, B. S.; Karnatchevich, V. L. *Russ. Chem. Bull*. **2004**, *53*, 2056. (e) Konarev, D. V.; Khasanov, S. S.; Saito, G.; Otsuka, A.; Lyubovskaya, R. N. *J. Mater. Chem*. **2007**, *17*, 4171. (f) Konarev, D. V.; Khasanov, S. S.; Lyubovskaya, R. N. *Russ. Chem. Bull*. **2007**, *56*, 371.

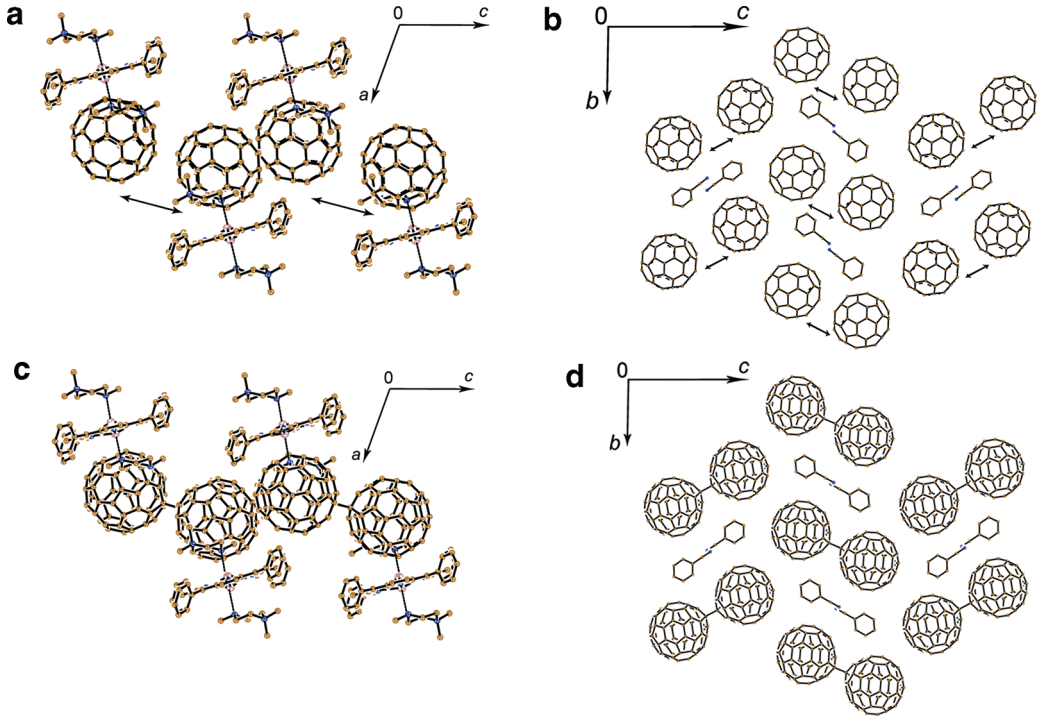

Figure 1. Crystal structure of **2**. View along and perpendicular to the fullerene layers for the monomeric phase at 270 K (a and b, respectively) and for the dimeric phase at 100 K (c and d, respectively). Arrows show the direction of dimerization.

five-coordinated in **1**. A similar geometry is observed for the $(TMP^+)_2 \cdot Mn^{II}TPP$ assemblies with essentially larger displacement of the Mn^{II} atoms out of the porphyrin plane [±0.4684(7) Å] and a shorter $Mn^{II}-N(TMP^+)$ bond of 2.493(2) Å (Figure 2b). The $Mn^{II}\cdots N(TMP^+)$ distance with the second TMP^+ cation is elongated to 3.424(4) Å. The average length of the equatorial $Mn^{II}-N(TPP)$ bonds is 2.123(2) Å. The close length of these bonds of 2.128(7) Å is observed in five-coordinated high-spin $Mn^{II}TPP \cdot Im$ units (Im = *N*-methylimidazole) with the displacement of the Mn^{II} atom from the plane of four nitrogen atoms by 0.56 Å.[13] It is known that only one ligand coordinates to $Mn^{II}TPP$ even in the presence of an excess of the ligand.[14] The coordination of two ligands to $Mn^{II}TPP$ is very rare and was found only in the coordination $(MDABCO^+)_2 \cdot Mn^{II}TPP$ units in the complexes with fullerenes. In this case, the length of the equatorial $Mn^{II}-N(TPP)$ bonds is shorter [2.081(2)−2.098(1) Å], and the Mn^{II} atoms locate in the porphyrin plane or slightly displace out of the porphyrin plane [±0.127(3) Å].[6a,b] Thus, the formation of a complex with C_{60} stabilizes the $(TMP^+)_2 \cdot M^{II}TPP$ assemblies. However, in spite of the fact that the environment of M^{II} in the porphyrins is favorable for the formation of six-coordinated metal species, they prefer coordination number 5.

The geometry of $(TMP^+)_2 \cdot Zn^{II}TPP$ remains almost unchanged in the dimeric phase at 100 K. The $M-N(TMP^+)$ bond is slightly shortened (Table 3), and a torsion angle between the lines passing through two nitrogen atoms of TMP^+ changes from 127.8(2)° at 250 K (Figure 2c) to 151.0(2)° at 100 K (Figure 2d). More pronounced changes are observed in the geometry of $(TMP^+)_2 \cdot Mn^{II}TPP$ at 100 K. The symmetry of the crystal structure of **2** decreases from monoclinic to triclinic under cooling. Asymmetry appears in the occupancies of two positions of Mn^{II}. One 84% occupied position has a smaller displacement of the metal atom out of the porphyrin plane [0.391(2) Å] and shorter axial and equatorial $Mn^{II}-N$ bonds, 2.425(3) and 2.114(3) Å, respectively. Another 16% occupied position of the Mn^{II} atom has a larger displacement of the metal atom out of the porphyrin plane [0.554(4) Å] and longer axial and equatorial $Mn^{II}-N$ bonds, 2.489(5) and 2.151(3) Å, respectively. The torsion angle between the lines passing through two nitrogen atoms of TMP^+ in the case of $(TMP^+)_2 \cdot Mn^{II}TPP$ slightly changes in the opposite direction from 128.5(2)° at 270 K to 122.6(2)° at 100 K.

d. Changes in the Magnetic Properties of 1 and 2 at Dimerization. The magnetic properties of polycrystalline **1** and **2** were studied by EPR and SQUID techniques. Complex **1** manifests a single line in the EPR spectrum with $g = 1.9994$ and $\Delta H = 3.84$ mT (see the Supporting Information). This signal was attributed to $C_{60}^{\bullet-}$. The line narrows with the temperature decrease, as was previously observed for the signals of $C_{60}^{\bullet-}$.[11c,d,15] Below 220 K, the signal intensity drops and the signal cannot be detected below 130 K. Only a weak narrow signal attributed to impurities is manifested down to 4 K. Such a transition indicates dimerization of $C_{60}^{\bullet-}$ and the formation of diamagnetic and EPR-silent single-bonded $(C_{60}^-)_2$ dimers[12e,15c] in agreement with X-ray diffraction data. The magnetic

(13) Kirner, J. F.; Reed, C. A.; Scheidt, W. R. *J. Am. Chem. Soc.* **1977**, *99*, 2557.

(14) Reed, C. A.; Kouba, J. K.; Grimes, C. L.; Cheung, S. K. *Inorg. Chem.* **1978**, *17*, 2666.

(15) (a) Paul, P.; Bolskar, R. D.; Clark, A. M.; Reed, C. A. *Chem. Commun.* **2000**, 1229. (b) Paul, P.; Kim, K.-C.; Sun, D.; Boyd, P. D. W.; Reed, C. A. *J. Am. Chem. Soc.* **2002**, *124*, 4394–4401. (c) Konarev, D. V.; Khasanov, S. S.; Saito, G.; Otsuka, A.; Yoshida, Y.; Lyubovskaya, R. N. *J. Am. Chem. Soc.* **2003**, *125*, 10074. (d) Konarev, D. V.; Kovalevsky, A. Yu.; Khasanov, S. S.; Saito, G.; Otsuka, A.; Lyubovskaya, R. N. *Eur. J. Inorg. Chem.* **2005**, 4822.

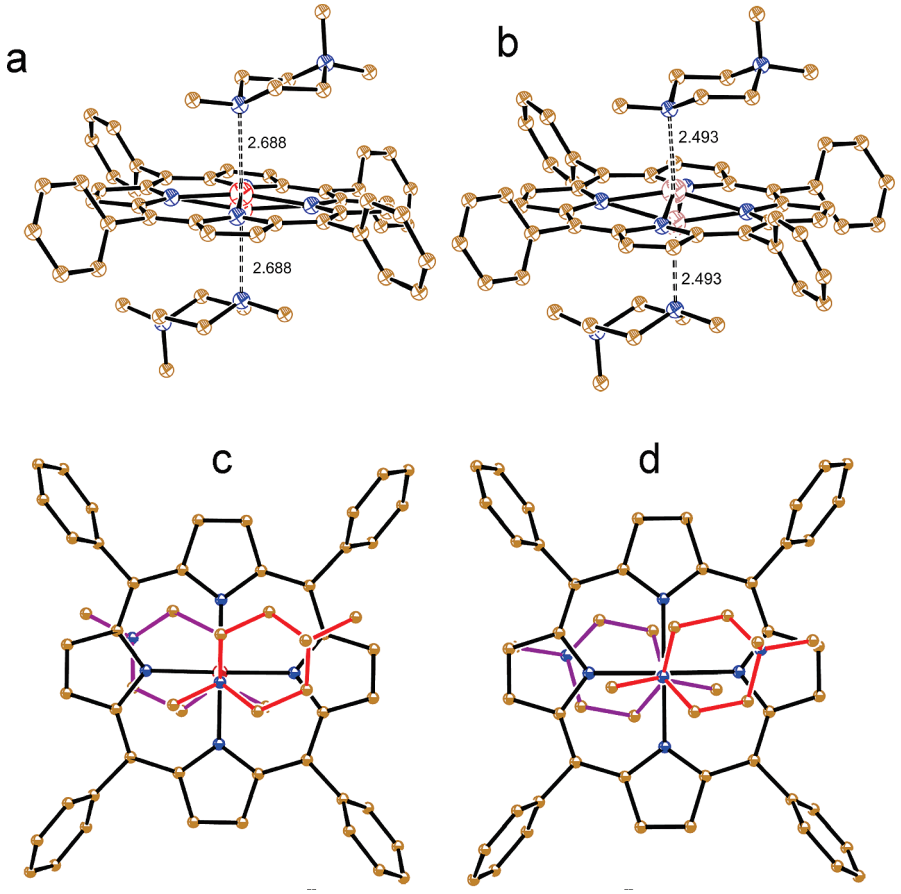

Figure 2. Geometries of $(TMP^+)_2 \cdot Zn^{II}TPP$ at 250 K (a) and $(TMP^+)_2 \cdot Mn^{II}TPP$ at 270 K (b). Views on the $Zn^{II}TPP$ macrocycle along the line passing through two coordinated nitrogen atoms of TMP^+ at 250 (c) and 100 K (d). The TMP^+ cations are shown in red and violet for clarity. The Zn−N(TMP^+) contacts are marked by dashed lines.

Table 3. Geometric Parameters for the $(TMP^+)_2 \cdot M^{II}TPP$ Assemblies in **1** and **2**

	1		**2**		
	100 K	250 K	100 K	200 K	270 K
Δ(M),[a] Å	±0.2309(12)	±0.2316(27)	0.3910(14) (84%), 0.5545(38) (16%)	±0.4567(7)	±0.4684(7)
M−N(TMP^+) bond length, Å	2.618(2)	2.688(3)	2.425(3) (84%), 2.489(5) (16%)	2.489(2)	2.493(2)
average M−N(TPP) bond length, Å	2.053(3)	2.054(3)	2.114(3) (84%), 2.151(3) (16%)	2.123(2)	2.123(2)
rms,[b] Å	0.0688	0.0493	0.0719	0.0498	0.0443

[a] Deviation of metal atoms from the mean plane of four nitrogen atoms. [b] Root-mean-square (rms) deviations of atoms from the mean plane of the porphyrin macrocycle.

moment of the complex is 2.41 μ_B at 300 K (Figure 3). The calculated magnetic moment for the system of two noninteracting ($S = {}^1/_2$) spins is 2.45 μ_B. Because the complex has two C_{60}^- anions per formula unit, both spins should be localized on fullerenes. The magnetic moment reversibly decreases below 230 K and is close to zero below 150 K (Figure 3). The observed paramagnetic−diamagnetic transition is due to $C_{60}^{\bullet -}$ dimerization. Below 100 K, less than 1% of spins from the total amount of C_{60} contribute to the magnetic susceptibility.

Complex **2** shows a high magnetic moment of 6.36 μ_B at 300 K. The calculated magnetic moment per formula unit containing a noninteracting $S = {}^5/_2$ spin from high-spin $Mn^{II}TPP$ and two $S = {}^1/_2$ spins from $C_{60}^{\bullet -}$ is 6.40 μ_B. The magnetic moment reversibly decreases in the 200−150 K range down to 6.00 μ_B. This value is close to the calculated magnetic moment of the system containing only noninteracting high-spin $Mn^{II}TPP$ (μ_{eff} = 5.92 μ_B). Thus, spins from $C_{60}^{\bullet -}$ disappear because of dimerization. Below 150 K, the Weiss temperature for **2** was estimated to be only −0.8 K, indicating that $(TMP^+)_2 \cdot Mn^{II}TPP$ assemblies are magnetically isolated by the diamagnetic $(C_{60}^-)_2$ dimers. Similarly, magnetic isolation of high-spin $(MDAB\text{-}CO^+)_2 \cdot Mn^{II}TPP$ was previously observed at the formation of complexes with diamagnetic single-bonded $(C_{70}^-)_2$ dimers[6a] or C_{60}^{2-} dianions.[6b]

Complex **2** manifests a broad room-temperature signal, which can be fitted by three Lorentzian lines with g_1 = 4.2200 (ΔH = 69.2 mT), g_2 = 2.9426 (ΔH = 81 mT), and g_3 = 2.0678 (ΔH = 111.6 mT) (Figure 4; see also the Supporting Information). The integral intensity of the component with g_3 is more than 3 times higher than those of both components with g_1 and g_2. The signal can be attributed to paramagnetic $(TMP^+)_2 \cdot Mn^{II}TPP$ and

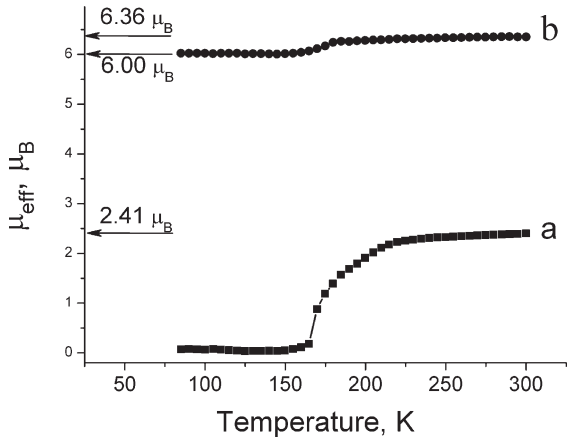

Figure 3. Temperature dependence of the magnetic moments for polycrystalline **1** (a) and **2** (b).

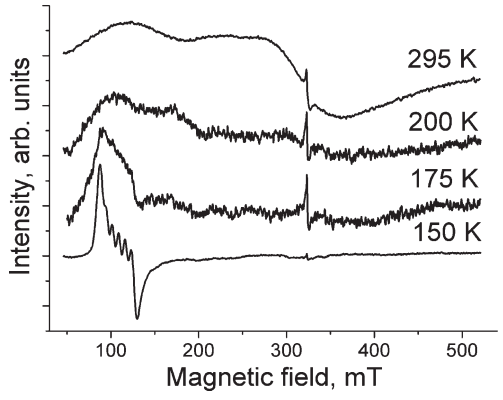

Figure 4. Evolution of the EPR spectrum of polycrystalline **2** with a temperature decrease.

$C_{60}^{\bullet-}$ species having strong exchange interaction. As a result, lines with *g*-factor values intermediate between those characteristic of $C_{60}^{\bullet-}$ and high-spin $Mn^{II}TPP$ are observed instead of separate lines from the individual species. Previously studied complexes containing $C_{60}^{\bullet-}$ and high-spin Mn^{II}porphyrins also show EPR spectra with two components observed at higher and lower magnetic fields. In $\{(MDABCO^+)\cdot Mn^{II}OEP\}\cdot(C_{60}^{\bullet-})\cdot(Solvent)_x$, two main components are manifested with $g_1 = 5.46$ ($\Delta H = 60$ mT) and $g_2 = 2.3418$ ($\Delta H = 40$ mT).[6e] The $\{(MDABCO^+)_2\cdot Mn^{II}TPP\}\cdot(C_{60}^{\bullet-})_2\cdot(Solvent)_x$ complex shows an asymmetric broad signal with a *g* factor close to 2.4 at room temperature. The signal shifts to higher values with a temperature decrease and $g = 4.9$ at 4 K.[6a] A narrow signal at 323.58 mT (Figure 4) can be attributed to monomeric $C_{60}^{\bullet-}$ radical anions ($g = 1.9964$ and $\Delta H = 4.51$ mT). The integral intensity of this signal is very low as compared with the integral intensity of the broad signal. Probably this signal originates from impurities.

Dimerization affects the EPR spectrum of **2** (Figure 4). Below 150 K, when dimerization is accomplished, a new signal characteristic of isolated high-spin $Mn^{II}TPP$ is manifested instead of the broad signal. The signal is asymmetric with a six-line hyperfine structure for ^{55}Mn ($I = {}^5/_2$; the average hyperfine coupling constant $|A|$ is 7.3 mT) and is centered at $g_\perp = 6$ and $g_{||} \approx 2$. Similar signals were previously observed for isolated high-spin $Mn^{II}TPP\cdot(C_6H_5CH_3)_2$ or $L\cdot Mn^{II}TPP$[14] (L = pyridine, 1-methylimidazole, and 2-methylimidazole) as well as in the $\{(MDABCO^+)_2\cdot Mn^{II}TPP\}\cdot\{(MDABCO^+)_2\cdot(C_{70}^-)_4\cdot(Solvent)_x$ complex containing diamagnetic single-bonded $(C_{70}^-)_2$ dimers.[6a]

Conclusion

Novel complexes containing metalloporphyrins and fullerene anions, $\{(TMP^+)_2\cdot M^{II}TPP\}\cdot(C_{60}^-)_2\cdot(C_6H_4Cl_2)_2\cdot(C_6H_5CN)_2$ [M = Zn (**1**) and Mn (**2**)], were obtained. Neutral metalloporphyrins are involved in the ionic fullerene complexes because of the formation of weak coordination $M-N(TMP^+)$ bonds. Complexes have layered structures. Fullerene layers contain pairs with short center-to-center interfullerene distances, which allow dimerization of the $C_{60}^{\bullet-}$ radical anions at 220−150 K in **1** and at 200−150 K in **2**. That results in the magnetic transition of **1** from the paramagnetic to diamagnetic state and a decrease of the magnetic moment of **2**. The latter transition is accompanied by changes in the shape of the EPR signal. The shape of the room-temperature signal is defined by an exchange interaction between $C_{60}^{\bullet-}$ and high-spin $(TMP^+)_2\cdot Mn^{II}TPP$. The disappearance of spins from $C_{60}^{\bullet-}$ at the formation of diamagnetic $(C_{60}^-)_2$ dimers restores the asymmetric signal characteristic of isolated high-spin $Mn^{II}TPP$. Two TMP^+ cations located above and below the porphyrin plane in $(TMP^+)_2\cdot M^{II}TPP$ allow the formation of six-coordinated metal species. However, metal atoms form a coordination bond only with one of two cations. As a result, metal atoms displace out of the porphyrin plane and are located above and below the porphyrin plane with equal occupancies for both positions. A structural transition takes place in **2** under cooling. The *C*2/*c* symmetry of the monoclinic lattice decreases to a triclinic one, and two positions of Mn^{II} become unequally occupied at 100 K, more obviously demonstrating the five-coordinated tendency for the metal atoms in $Mn^{II}TPP$. On the whole, the complexes are fascinating examples of ionic metalloporphyrin−fullerene architectures obtained via coordination and electrostatic interactions between the components. The complexes show unusual magnetic and structural transitions.

Acknowledgment. The work was supported by the RFBR (Grants 09-02-01514 and 10-03-00787), MEXT Japan (Grant 20110006), and JSPS (Grant 18GS0208).

Supporting Information Available: X-ray crystallographic data in CIF format. This material is available free of charge via the Internet at http://pubs.acs.org.